Title	A comprehensive combustion chemistry study of 2,5-dimethylhexane
Author(s)	Sarathy, S. Mani; Javed, Tamour; Karsenty, Florent; Heufer, Alexander; Wang, Weijing; Park, Sungwoo; Elwardany, Ahmed; Farooq, Aamir; Westbrook, Charles K.; Pitz, William J.; Oehlschlaeger, Matthew A.; Dayma, Guillaume; Curran, Henry J.; Dagaut, Philippe
Publication Date	2014-01-16
Publication Information	Sarathy, SM,Javed, T,Karsenty, F,Heufer, A,Wang, W,Park, S,Elwardany, A,Farooq, A,Westbrook, CK,Pitz, WJ,Oehlschlaeger, MA,Dayma, G,Curran, HJ,Dagaut, P (2014) 'A comprehensive combustion chemistry study of 2,5-dimethylhexane'. Combustion And Flame, 161 :1444-1459.
Publisher	Elsevier ScienceDirect
Link to publisher's version	http://dx.doi.org/10.1016/j.combustflame.2013.12.010
Item record	http://hdl.handle.net/10379/6145
DOI	http://dx.doi.org/10.1016/j.combustflame.2013.12.010

Comprehensive experimental and kinetic modeling study of 2,5-dimethylhexane, an iso-paraffinic surrogate for transportation fuels

S. Mani Sarathy[1*], Tamour Javed[1], Florent Karsenty[2], Alexander Heufer[3], Weijing Wang[4], Sungwoo Park[1], Ahmed Elwardany[1], Aamir Farooq[1], Charles K. Westbrook[5], William J. Pitz[5], Matthew A. Oehlschlaeger[4], Guillaume Dayma[2], Henry J. Curran[3], Philippe Dagaut[2]

[1] Clean Combustion Research Center, Division of Physical Sciences and Engineering, King Abdullah University of Science and Technology, Thuwal 23955-6900, Saudi Arabia
[2] CNRS-INSIS, 1C, Ave de la Recherche Scientifique, Orleans Cedex 2, France
[3] Combustion Chemistry Centre, School of Chemistry, National University of Ireland Galway, Ireland
[4] Mechanical, Aerospace, and Nuclear Engineering, Rensselaer Polytechnic Institute, Troy, NY, USA
[5] Lawrence Livermore National Laboratory, Livermore, CA, USA

*Corresponding Author:
S. Mani Sarathy
mani.sarathy@kaust.edu.sa
Clean Combustion Research Center, King Abdullah University of Science and Technology
Thuwal 23955-6900
Kingdom of Saudi Arabia

Abstract

Iso-paraffinic molecular structures larger than seven carbon atoms in chain length are commonly found in conventional petroleum, Fischer–Tropsch (FT), and other alternative hydrocarbon fuels, but little research has been done on their combustion behavior. Recent studies have focused on either mono-methylated alkanes and/or highly branched compounds (e.g., 2,2,4-trimethylpentane). In order to better understand the combustion characteristics of real fuels, this study presents new experimental data for the oxidation of 2,5-dimethylhexane under a wide variety of temperature, pressure, and equivalence ratio conditions. This new dataset includes jet stirred reactor speciation, shock tube ignition delay, and rapid compression machine ignition delay, which builds upon recently published data for counterflow flame ignition, extinction, and speciation profiles. The low and high temperature oxidation of 2,5-dimethylhexane has been modeled using a comprehensive chemical kinetic model developed using established reaction rate rules. The agreement between the model and data is presented, along with suggestions for improving model predictions. The importance of propene chemistry is highlighted as critical for correct prediction of high temperature ignition delay. The oxidation behavior of 2,5-dimethylhexane is also compared with oxidation behavior of other linear and branched octane isomers, in order to determine the effects of the number of methyl branches on combustion properties. Both experimental data and model predictions indicate that increasing the level of branching decreases fuel reactivity at low and intermediate temperatures. The model is used to elucidate the structural features and reaction pathways responsible for inhibiting the reactivity of 2,5-dimethylhexane.

Introduction

Detailed chemical kinetic models for transportation fuels have reached a level of fidelity where accurate predictions can be made of combustion phenomenon relevant to the operation of practical devices. Schofield [1] states that these large scale models are adequate as engineering tools for studying the combustion of new fuel molecules. A recent review paper by Pitz and Mueller [2] describing the development of diesel surrogate fuel models concluded that major research gaps remain in modeling high molecular weight (i.e., C_8 and greater) aromatics, alkyl aromatics, cyclo-alkanes, and lightly branched *iso*-alkanes. The present study is concerned with the combustion of branched alkanes, specifically 2,5-dimethylhexane, which has been reported as a component of petroleum combustion exhaust, smog, and tobacco smoke [3]. Branched alkanes are important components of conventional diesel and jet fuels derived from petroleum [2,4]; synthetic Fischer-Tropsch diesel and jet fuels derived from coal, natural gas, and/or biomass [5,6]; and renewable diesel and jet fuels derived from thermochemical treatment of bio-derived fats and oils (e.g., hydrotreated renewable jet (HRJ) fuels) [7,8]. Detailed compositional reports by Bruno and coworkers [8,9] for turbine fuels, such as GTL, CTL, SPK, and biomass-derived fuels indicate that di-methylated alkanes represent an important fraction of the fuel composition. Huber et al. [10] have also proposed 2,6-dimethyloctane as a surrogate component for synthetic aviation fuel S-8.

The present study on di-methylated alkane combustion builds upon previous experimental and modeling work performed by the authors on the combustion of branched alkanes [11-16] . The team has recently provided a wealth of experimental data spanning low-temperature auto ignition delay times to high-temperature premixed flame propagation rates for several octane isomers, together with chemical kinetic models capable of predicting the experimental data. The ultimate goal is to develop a body of experimental data and kinetic models, which can be used to better understand combustion of branched alkanes and to develop surrogates for the combustion of real fuels with iso-paraffinic fractions. The feasibility of using di-methylated alkanes as surrogates for real fuels is uncertain. One constraining factor is their high cost, which makes it expensive to run large-scale combustion experiments. Dooley et al. [17] showed that a less expensive mixture of n-decane and iso-octane (2,2,4-trimethylpentane) is an appropriate surrogate for a synthetic paraffinic jet fuel (i.e., S-8) rich in mono-methylated alkanes because the real fuel's "distinct chemical functionalities" [17] are captured in the surrogate. On the other hand, Mueller et al. [18] concluded that utilizing large iso-alkanes representative of those found in real fuels could be advantageous. In a recent study on the ignition of JP-8 and hydrotreated renewable jet fuels, Allen et al [19] utilized surrogates principally composed of large mono-methylated alkanes [20] in chemical kinetic modeling simulations to predict combustion behavior of the real fuels. They suggested that utilizing a di-methylated alkane as a surrogate for the real fuels could improve predictability, if accurate chemical kinetic models were available.

Recent comprehensive experimental and modeling studies on 2-methylheptane and 3-methylheptane [11-13,16,20] have shown that mono-methylated alkanes exhibit notably different combustion properties than their linear alkane counterparts (e.g., n-octane), including lower laminar flame speeds and decreased low temperature reactivity. Prior fundamental combustion

studies on di-methylalkanes are limited. Sarathy et al. [13] conducted an experimental and numerical study on counterflow diffusion flames of 2,5-dimethylhexane, and observed a decreased propensity for flame ignition and an increased propensity towards flame extinction when compared to mono-methyl and normal octane isomers. Liu et al. [14] studied C_8 and C_{10} di-methylated alkane ignition in non-premixed flames and found similar trends, wherein di-methylalkanes were found to be less reactive than isomeric normal and mono-methylated alkanes. Ji et al. [15] conducted experimental laminar flame speed measurements of five octane isomers (including 2,5-dimethylhexane) and compared them to chemical kinetic modeling predictions; both experimental and modeling results indicated that 2,5-dimethylhexane exhibits lower laminar flame speeds than mono-methylated octane isomers, thereby suggesting that increasing the number of methyl substitutions decreases reactivity. High-temperature combustion in flames is dominated by a fuel's ability to populate the hydrogen radical pool, and chemical kinetic modeling simulations [13,15] indicate that the decreased reactivity of 2,5-dimethylhexane in flames is due to its decreased ability to populate the H-atom radical pool.

The chemistry is different in low and intermediate temperature combustion systems wherein the competition between primary OH branching and OH propagation pathways controls fuel reactivity. In a rapid compression machine ignition study of the heptane isomers ($\varphi = 1$, P = 15 atm, 650 K to 950 K), Silke et al. [21] showed that di-methylated heptane isomers exhibit lower reactivity when compared to mono-methylated and normal heptane isomers. In a series of comprehensive kinetic modeling studies on the autoignition of heptane isomers, Westbrook et al. [22,23] also showed that the reactivity of di-methylated heptane isomers was lower than that of mono-methylated and normal heptane isomers at low and intermediate temperatures; however, at higher temperatures, their model predicted that all heptane isomers display the same ignition characteristics, which was later confirmed experimentally by Smith et al. [5]. Not surprisingly, the aforementioned studies showed that the ignition behavior of heptane isomers in the negative temperature coefficient (NTC) region correlates with the research octane number (RON) of the fuel, which was also shown by Morley [24].

The objective of the current study is to present new experimental data for 2,5-dimethylhexane oxidation in a jet stirred reactor (JSR), rapid compression machine (RCM), and shock tube (ST) at conditions similar to those previously studied for mono-methylated and normal octanes [11,16,20]. The experimental data is used to compare the reactivity of the symmetrical di-methylated octane fuel with other octane isomers. Furthermore, a comprehensive detailed chemical kinetic combustion model is developed for 2,5-dimethylhexane oxidation. The model is then used to understand the effect of multiple methyl branches on important combustion phenomenon. This 2,5-dimethylhexane study also aids in testing the selected reaction pathways and rate rules; thus providing a methodology for which similar models could be built for larger di-methylalkanes found in conventional and alternative transportation fuels.

Chemical kinetic modeling

The proposed detailed chemical kinetic reaction mechanism includes high-temperature kinetic pathways for 2,5-dimethylhexane [13], plus low-temperature kinetic schemes for 2,5-dimethylhexane. The reactions were added to the recently developed 2-methylheptane and 3-

methylheptane high-temperature oxidation schemes presented by LLNL [11,16,20]. The same reaction classes and rate rules were used as previously discussed for branched alkanes [20]. The C_0-C_5 base chemistry employed here is the Aramco Mech 1.3 developed at NUI Galway [25].

Naming of species

To illustrate the naming of the species for the mechanism, 2,5-dimethylhexane is denoted as C_8H_{18}-25 in the mechanism, for example (see Figure 1 for its molecular structure). The carbon chain is labeled numerically (i.e., 1, 2, 3) such that the location number of the methyl branch is minimized. For 2,5-dimethylhexene species, the location of a double bond is identified by another hyphen identifying the location of the double bond (e.g., 2,5-dimethyl-2-hexene is C_8H_{16}-25-2). Additional notations are provided to denote radical sites in the molecule, wherein the carbon sites are labeled alphabetically (i.e., a, b, c) such that the location of the first methyl branch is minimized (Figure 1). In this way, the 2,5-dimethyl-2-hexyl radical is denoted as C_8H_{17}-25b, while the 25-dimethyl-1-hexyl radical is written as C_8H_{17}-25a.

Classes of reactions, rate constant rules, and thermochemical data

The major classes of elementary reactions considered for the oxidation of 2,5-dimethylhexane include 10 high temperature reaction classes and 20 low-temperature reaction classes. These reaction classes and the selected reaction rate rules for branched alkanes have been described in detail previously [20]. The rate rules established for normal and mono-methylated alkanes caused ignition delay times for 2,5-dimethylhexane to be under predicted. Therefore, following previous work on *iso*-octane (2,2,4-trimethylpentane) modeling [26], the A-factors for six-membered ring H-atom migrations from primary and tertiary sites were reduced by a factor of 3 for RO_2 to QOOH isomerization reactions (class 23) and the O_2QOOH isomerizations to carbonylhydroperoxide + OH (class 27). This was done only for peroxy radicals derived from 2,5-dimethylhexane and not for small alkylperoxy radicals. The A-factors for H-atom abstractions by HO_2 radical were increased by a factor of 3 to provide better agreement with measured ignition delay times measured at 900 to 1200 K. The previously used rate constants [20] were from the quantum-level calculations of Aguilera-Iparraguirre et al. [27], whereas the new rate constants are in closer agreement with the calculations of Carstensen and Dean [28].

An accurate propene sub-mechanism is important for correctly predicting 2,5-dimethylhexane ignition delay times above 1200 K, as will be discussed in further detail later in this manuscript. A factor of 5 increase in the rate constant for $C_3H_5 + HO_2 \leftrightarrow C_3H_5O + OH$ was needed to match the measured ignition delay times for 2,5-dimethylhexane. This rate constant modification increases the overall oxidation of propene, and thus enhances the reactivity of 2,5-dimethylhexane at high temperatures. This rate constant modification should not be adopted universally. The authors acknowledge that high temperature propene oxidation chemistry is an area of research that warrants further investigation, and are aware of separate efforts to improve the AramcoMech propene sub-mechanism based on more comprehensive propene oxidation and pyrolysis studies [29].

The thermodynamic parameters for the species are very important because they are used to determine reverse rate constants. The THERM [30] software was used to compute the

thermochemical properties of species not present in the 2-methylalkanes model. The THERM group values are from Benson [31] and Bozzelli [32].

It is noted that the combustion model for 2,5-dimethylhexane, prior to the aforementioned modifications, has been validated under high temperature conditions against premixed laminar flame speeds [15] and counterflow flame data [13]. The slightly modified model presented here also well predicts high temperature premixed flame propagation rates and diffusion flame extinction, ignition, and species profiles. The present study extends the model validation to low-, intermediate-, and high-temperature ignition delay and oxidation speciation targets under premixed stirred reactor conditions. These experiments allow for a more comprehensive validation of the oxidation pathways, including concerted elimination reactions leading to alkene formation and reactions producing cyclic ethers.

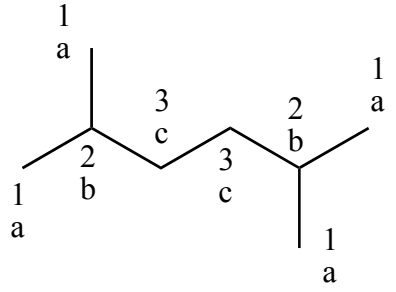

Figure 1 – Carbon skeletal structure of 2,5-dimethylhexane (C_8H_{18}-25) with carbon sites labeled

Model validation studies

The proposed model for the 2,5-dimethylhexane is validated against a wide range of experimental data covering low-temperature and high-temperature oxidation conditions. The following is a list of specific validation targets presented in this study:

1. Ignition delay data from a ST at King Abdullah University of Science and Technology at equivalence ratios of 0.5, 1.0, and 2.0, temperatures in the range of 1100 K to 1500 K, and pressures of 5 and 10 atm.
2. Ignition data from a ST at Rensselaer Polytechnic Institute at equivalence ratios of 0.5, 1.0, and 2.0, temperatures ranging from 698 to 1255 K, and nominal pressures of 20 and 40 atm
3. Ignition data from an RCM at National University of Ireland in Galway at pressures near 5 and 10 atm, temperatures range of 574 to 1062 K, and equivalence ratios of 0.5, 1.0 and 2.0.
4. Concentration profiles from a JSR at CNRS Orleans operating at 10 atm, constant residence time, τ, of 0.1 s, a range of equivalence ratios from 0.5 to 2, and temperatures from 550 to 1150 K.

Experimental methodologies

Shock tube ignition measurements in Ar (KAUST)

High temperature ignition delay time measurements were performed in the Low Pressure Shock Tube (LPST) at King Abdullah University of Science and Technology (KAUST). This is an ultra-high purity shock tube constructed from stainless steel where the inner surface is electropolished

to reduce boundary layers and to reduce potential out-gassing of impurities from porous walls. The inner diameter of the shock tube is 14 cm; it consists of 9 meter long driven section, and the length of the driver section can be varied (maximum 9 meter) depending on the required test times. These dimensions of the shock tube enable long test times (~50 ms) using contact surface tailoring; see [33,34] for contact surface tailoring theory. The driver and driven sections are separated by a polycarbonate diaphragm. The diaphragm is ruptured by a cross-shaped cutter blade configuration when the driver section is filled by the driver gas (usually Helium). The rupturing diaphragm pressure P_4 can be varied by changing the diaphragm thickness and the cutter blade position.

Incident shock velocity was measured by using four PCB 113B26 piezoelectric pressure transducers (PZTs) that were located axially along the driven section. The signal from PZTs was used to trigger four ultra-fast (350 MHz) Agilent 53220A frequency counter/timer to determine the time interval between two successive pressure transducers. The counter outputs were used to get the axial incident shock velocity profile. The incident shock speed at the end-wall was determined by linear extrapolation of the velocity profile. The attenuation rates were less than 0.8% per m and the errors in calculated end-wall shock speed were less than 0.1% in all experiments. One-dimensional reflected shock equations were used to calculate the conditions (i.e., temperature, pressure) behind the reflected shock wave. The thermodynamic parameters used for Argon and Oxygen were taken from Sandia thermodynamic database [35] and for 2,5 dimethylhexane from [13]. Sidewall pressure history was measured using Kistler 603B1 PZT located at 2cm from the end-wall. At the same axial position, OH^* chemiluminescence associated with $A^2\sum^+ \rightarrow X^2\prod$ transition near 306 nm was detected by a lens/slit setup using a modified Thorlab PDA36A detector and narrow bandpass filter from Andover Corporation (centered at 306nm with FWHM<10nm). The optical setup for ignition delay time measurements, shown in **Figure 2**, was based on type II configuration as described by [36], which gives an axial spatial resolution of less than 5mm.

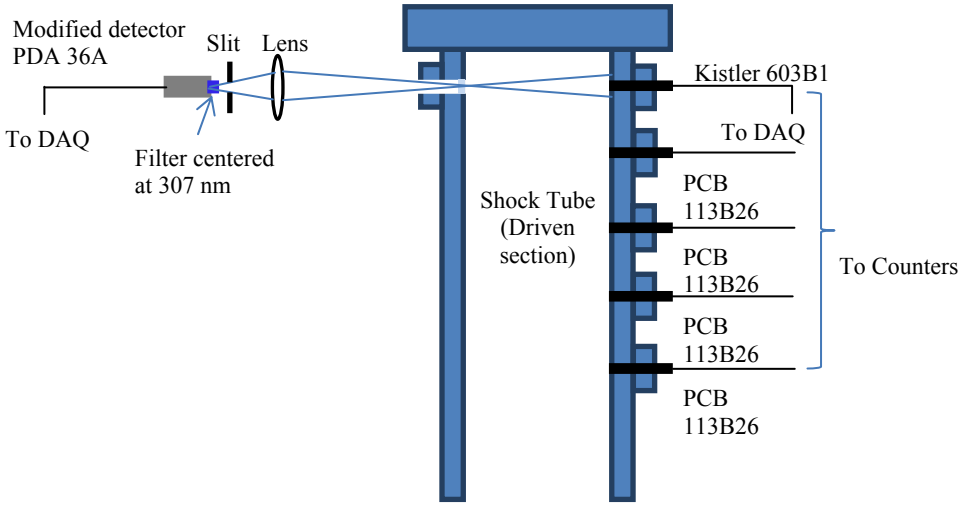

Figure 2 – Optical configuration for ignition delay measurements

In this study, ignition delay time is defined as the time interval between the arrival of the reflected shockwave and the onset of ignition at the observation location 2 cm from the shock tube end-wall (**Figure 3**). The arrival of the reflected shockwave (time zero) was determined by step rise in the pressure signal (response time of pressure transducer is less than 10μs). The onset of ignition was determined by extrapolating the steepest rise in both pressure and OH* chemiluminescence to the respective pre-ignition zero signal. Both methods agree well with each other (± 2%). More detailed discussion on different definitions of ignition delay can be found in [37].

Mixtures were prepared manometrically in a stainless steel mixing tank. This mixing tank is equipped with a magnetic stirrer which helps in expediting the mixing process and ensuring homogeneity of the mixture. Partial pressure of the fuel was always kept less than two-third of the room-temperature saturation vapor pressure to avoid condensation inside the mixing tank/shock tube. The mixing times varied from 1.5 hr to overnight; however, ignition delay time results showed no dependence on mixing time. The shock tube can be pumped down to 1 x 10^{-6} mbar using Varian TV 551 turbo pump by overnight pumping. A 30-minute pumping, used for these experiments, achieved a pressure of 2 x 10^{-3} mbar. Leak rate of the shock tube was found to be 5 x 10^{-6} mbar/min. The fuel studied (2,5 dimethylhexane) was obtained from Chemsampco and its purity was verified as discussed later. Ignition delay times were measured behind the reflected shock wave over the temperature range of 1100 K to 1500 K, pressures of 5 and 10 atm, and equivalence ratios of 0.5, 1 and 2 with Argon as the diluent. In all experiments, the concentration of the fuel was kept fixed at 0.4%. Research grade Ar and O_2 were used to make the desired mixtures and research grade Helium was used as driver gas in all experiments. Estimated uncertainty in ignition delay times is ± 17% owing mainly to the uncertainty in reflected shock temperature and mixture concentration.

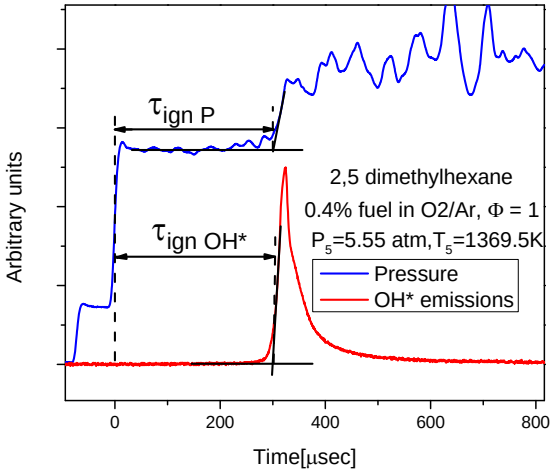

Figure 3 – Example 2,5 dimethylhexane ignition data in O_2/Ar showing ignition delay time definition

Shock tube ignition measurements in air (RPI)

Ignition delay time measurements for 2,5-dimethylhexane/air mixtures were carried out using the reflected shock technique in the Rensselaer heated high-pressure shock tube, described previously in [38]. 2,5-Dimethylhexane/air mixtures at equivalence ratios of 0.5, 1.0, and 2.0, where air was

defined as pure N_2 and O_2 (99.995% from Noble Gas) at a ratio of 3.76:1, were prepared in a heated (120-140°C) mixing vessel and mechanical mixed to ensure homogeneity prior to experiments. The shock tube was also maintained at a uniform heated temperature of 120-140°C to avoid fuel condensation.

Ignition delay times were measured by monitoring pressure at a side wall location 2 cm from the shock tube driven section end wall and chemiluminescence from electronically-excited hydroxyl radicals (OH*) viewed through the driven section end wall with a filtered photodetector. Ignition delay times were defined as the time interval between shock reflection at the end wall and the onset of ignition at the end wall, defined by extrapolating the maximum slope in OH* chemiluminescence to the baseline detector signal; see Figure 4 for an example ignition delay time measurement. Following the passage of the reflected shock wave the pressure was observed to slowly rise due to viscous gas dynamics at a rate of $(dP/dt)(1/P_0) = 2 – 3\%\ ms^{-1}$, which is incorporated into kinetic modeling simulations. The uncertainty in ignition delay is ±20% (95% confidence interval), where the majority of ignition delay uncertainty stems from uncertainty in the reflected shock temperature.

Ignition delay measurements for $\varphi = 0.5$ and 1.0 mixtures were carried out at nominal pressures of 20 and 40 atm. For $\varphi = 2.0$, measurements were only carried out at 20 atm. The total temperature range for these elevated pressure 2,5-dimethylhexane/air ignition delay measurements, from 698 to 1255 K, spans the low-temperature, NTC, and high-temperature regimes of reactivity and includes ignition delay times from 46 μs to 7.4 ms. Ignition delay times in excess of ~1.5 ms were enabled through the use of driver gas tailoring (N_2/He mixtures) to extend reflected shock test time. All ignition delay times can be found in the appended supplementary material.

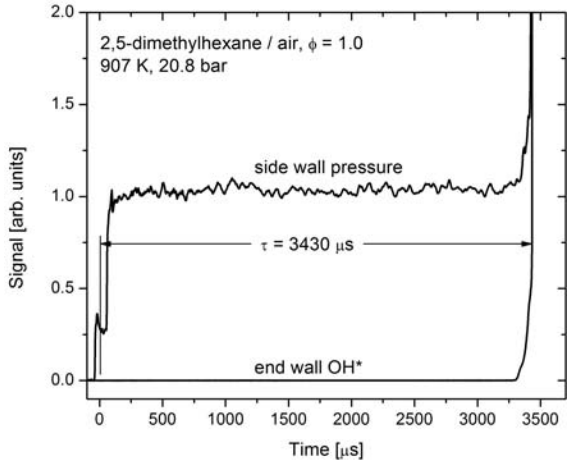

Figure 4 - Example 2,5-dimethylhexane/air ignition delay time measurement.

Rapid compression machine ignition

Experiments have been performed in a double piston rapid compression machine. By the opposed movement of two twin pistons compression times below 16 ms are achieved. The diameter of the

reaction chamber is 38.2 mm and special care has been taken ensuring a homogenous pre-heating of the reaction chamber which is possible up to 160°C. Besides the purpose of avoiding fuel evaporation in the case of liquid fuels, pre-heating of the combustion chamber is used to alter the initial temperature before compression subsequently allowing varying the temperature at the end of compression. Furthermore, it is possible to change the conditions at the end of compression by varying the initial pressure, the diluents gas composition, and the volumetric compression ratio. In the present study the variation of compression ratio was not necessary to cover the whole range of conditions of interest.

Experiments have been performed at 5 and 10 atm for two equivalence ratios, i.e. $\varphi = 0.5$, $\varphi = 1.0$ and $\varphi = 2.0$. For all experiments the oxygen:diluent ratio was 21:79. Experiments at lowest temperatures have been performed with 62.5% CO_2 + 37.5% N_2 as diluents and at highest temperatures 80% Ar and 20% N_2 for $\varphi = 0.5$ and $\varphi = 1.0$ and 100 % Ar for $\varphi = 2.0$ have been used. For the intermediate temperature regime pure nitrogen as diluent has been chosen. All mixtures have been prepared in separate heated stainless steel mixing vessels. Mixture composition has been controlled by measuring partial pressures assuming ideal mixing of the gases.

For accurate simulation of RCM experiments the volume history of the experiments has to be included in simulation. The volume histories for the different mixtures are deduced from pressure measurements performed with non-reactive mixtures. For these non-reactive mixtures the oxygen has been replaced by nitrogen.

The ignition delay time is defined as the time difference between the end of compression indicated by the first maximum in the pressure profile and the ignition event. The ignition time is read at the maximum pressure gradient. Analogously, the first stage ignition delay time is defined as the time difference between the end of compression and the maximum pressure rise due to the first stage ignition (see Figure 5).

Uncertainties in the RCM measurements have been estimated in detail in a previous study [39,40]. From this study it is assumed the uncertainty in the pressure measurement is ±0.5 atm and the uncertainty in the end of compression temperature ±5 K. In all experiments (i.e., reactive and non-reactive) the difference in the piston displacement profiles was below 1 ms.

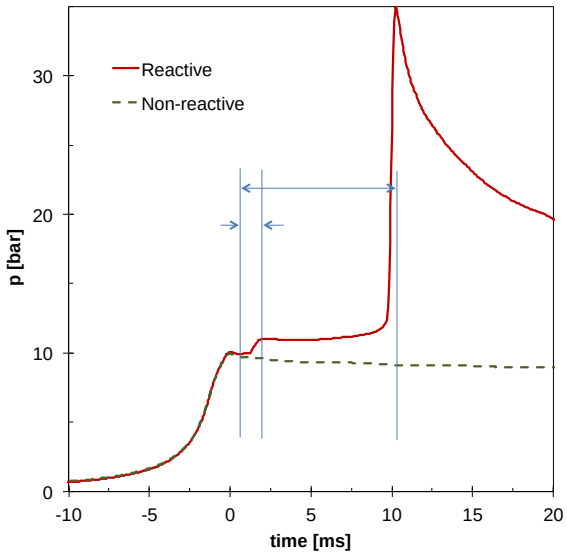

Figure 5 - Comparison of reactive and non-reactive experiment, definition of ignition delay times, stoichiometric condition with 100 % N_2 diluent.

Jet stirred reactor

We used the JSR experimental setup utilized in previous studies [20,41]. It consisted of a small spherical fused-silica reactor (4 cm outside diameter) equipped with four nozzles of 1 mm inner diameter (ID) each. High-purity reactants were used: oxygen (99.995% pure) and 2,5-dimethylhexane (CAS 592-13-2, >98.1% pure from ChemSampCo). The reactants were diluted with nitrogen (<50 ppm H_2O) and quickly mixed before admission into the 4 injectors. The reactants were preheated to minimize temperature gradients within the reactor. A Shimadzu LC10 AD VP pump operating with an on-line degasser (Shimadzu DGU-20 A3) was used to distribute the fuel to a in-house atomizer-vaporizer assembly thermally regulated at 473 K. A high degree of dilution (1000 ppm of fuel) was used to reduce heat release and minimize temperature gradients inside the reactor (ca. 1 K/cm along the vertical axis of the JSR measured by a 0.1 mm Pt-Pt/Rh-10% thermocouple protected by a thin-wall silica tube to avoid catalysis). A movable low-pressure sonic probe (made of fused silica) was used to suck samples of the reacting mixtures from the JSR. The samples were transferred to several analyzers via a temperature-controlled heated line (473 K). They were analyzed online by FTIR (200 mbar; 10m path length; spectral resolution of 0.5 cm-1) and off-line, after collection in 1 L Pyrex bulbs at ca. 50 mbar. Gas chromatographs (GC) equipped with capillary columns (DB-624 for oxygenates and >C5 hydrocarbons, CP-Al2O3-KCl for hydrocarbons, and Carboplot-P7 for hydrogen and oxygen), a thermal conductivity detector, and a flame ionization detector were used for off-line analyses. The identification of products was performed by means of a GC-MS (V1200 from Varian) operated with electron ionization (70 eV).

The experiments were performed at steady state, at a constant pressure of 10 atm and a constant mean residence time of 0.7 s. The reactants flowed continuously into the JSR and the temperature of the gases inside the reactor was increased stepwise. A good repeatability of the measurements and a reasonably good C-balance (typically 100 ± 12%) were determined. The accuracy of

concentration measurements was ca. ± 15%, in reactor temperature was ± 5 K and in reactor residence time is ± 0.02 s.

Results and Discussion

Verification of fuel quality

The 2,5-dimethylhexane fuel used in all the experiments was provided by ChemSampCo (Texas, USA) with a stated purity of >98.1%. However, the supplier was unable to provide a certificate of analysis that the octane fuel isomer was 2,5-dimethylhexane because conventional gas chromatography/mass spectrometry (GC/MS) methods cannot differentiate between all octane isomers. Thus, the fuel quality was tested using nuclear magnetic resonance (NMR) facilities available at KAUST. NMR techniques are useful for identifying the number of hydrogen atoms attached to carbon atoms, and therefore can be used to identify and quantify functional groups in a fuel sample [4]. The sample was prepared by dissolving the fuel in 1 mL of deuterated chloroform $CDCl_3$ and then 0.6 ml of the solution was transferred to 5 mm NMR tubes. NMR spectra were acquired at 298 K using Bruker 600 AVANAC III spectrometer equipped with Bruker BBO multinuclear probe. The ^1H NMR spectra were recorded by collecting 64 scans with a recycle delay time of 5 s, using standard 1D 90° pulse sequence using standard (zg) program from Bruker pulse library. Chemical shifts were referenced to internal tetramethylsilane (0 ppm) or to internal residual $CHCl_3$ in solvent $CDCl_3$ (7.23 ppm). Exponential line broadening of 1 Hz was applied before Fourier Transformation. Bruker Topspin 2.1 software was used in all experiments to collect and analyze the data.

The 2,5-dimethylhexane is a symmetric compound, so is expected to give three signals in the NMR. The resulting NMR spectrum for the fuel sample is shown in **Figure 6**. A methyl signal (CH_3) exists near 0.9 ppm corresponding to 4 CH_3 groups. A methylene (CH_2) signal near 1.1 ppm indicates that there are 2 CH_2 groups. Finally, a signal related to the methylidyne (CH) is observed near 1.5 ppm indicating 2 CH groups. Therefore, the structure is 2,5-dimethylhexane and the purity is expected to be ≥ 98 %.

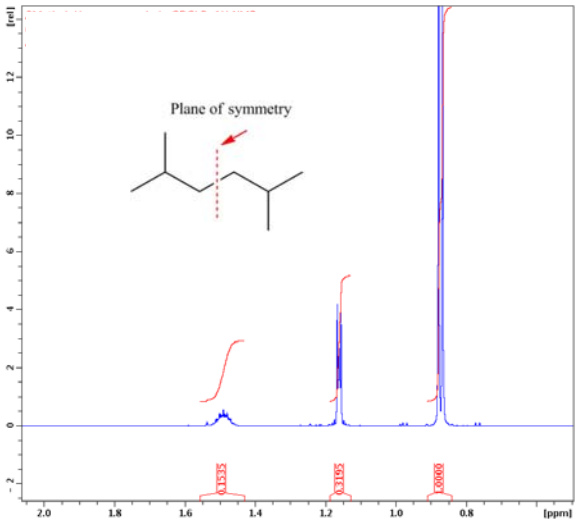

Figure 6 – NMR ^1H spectrum of 2,5-dimethylhexane

Shock tube ignition measurements in Ar

High temperature ignition delay time measurements performed in the LPST at KAUST are presented in **Figure 7** and **Figure 8**. The effect of equivalence ratio on ignition delay times was determined by measuring ignition delay times for fuel lean, stoichiometric and fuel rich mixtures (Φ = 0.5, 1, 2). The equivalence ratio was varied by changing the O_2 concentration with a fixed fuel concentration. It was found that the fuel lean mixtures were easiest to ignite and fuel rich mixtures were least reactive. This is due to the fact that the dominant chain branching reaction in high temperature regime $H + O_2 \rightarrow O + OH$ is directly linked to the concentration of molecular oxygen which is highest in the lean mixture. It is known that the high-temperature ignition delay times of alkanes in a shock tube are a strong function of oxygen concentration (Olchanski and Burcat, Decane Oxidation in a

Shock Tube, IJCK2006) The effect of pressure on ignition delay times was studied by performing experiments at 5 and 10 atm. Reactivity increases by increasing the pressure, i.e. the higher the pressure, the shorter the ignition delay. **Figure 9** illustrates the effect of pressure on ignition delay for Φ=0.5 case and same conclusion can be drawn for other equivalence ratios. Pressure scaling of ignition delay data was found to be $\tau_{ign} \propto p^{-0.74}$.

The LPST Ignition delay was modeled with CHEMKIN PRO [42] with an imposed volume history to account for the experimentally measured pressure gradient, $dP/dt(1/P_0)$ = 3.5% ms^{-1}. Initial simulations employed the high temperature chemical kinetic model published previously [13], which consists of 3401 reactions involving 714 species. However, the model consistently over predicted ignition delay times at all experimental conditions. A sensitivity analysis was conducted to determine which reactions have a large effect on the ignition delay times of 2,5 dimethylhexane. Specifically, temperature sensitivity analysis was performed at the time of ignition using Chemkin Pro. Since there is a large change in temperature near the time of ignition, reactions that accelerate ignition exhibit a positive temperature sensitivity and those that slow ignition exhibit a negative sensitivity.The results are shown in Figure 10. Many of the sensitive reactions are related to propene chemistry because multiple methyl substitutions result in 2,5-dimethylhexane quickly decomposing to propene [13]. In order to accelerate propene oxidation, the rate of the propenyl reaction with hydroperoxyl ($C_3H_5+HO_2 \leftrightarrow C_3H_5O + OH$) was increased by a factor of 5 in the proposed model. Further experiments targeted on propene chemistry and direct rate measurements are needed to confirm the rate of this reaction and other related reactions shown in Figure 10. The model proposed herein improves agreement between experimental data and model, as shown in **Figure 7** and **Figure 8**. The qualitative effects of temperature, pressure, and equivalence ratio are well predicted by the proposed model. The quantitative predictions are generally within the experimental uncertainty limit of ± 17%, but a greater discrepancy (i.e., factor of 2) is observed for the highest temperatures of the 5 atm stoichiometric and rich data.

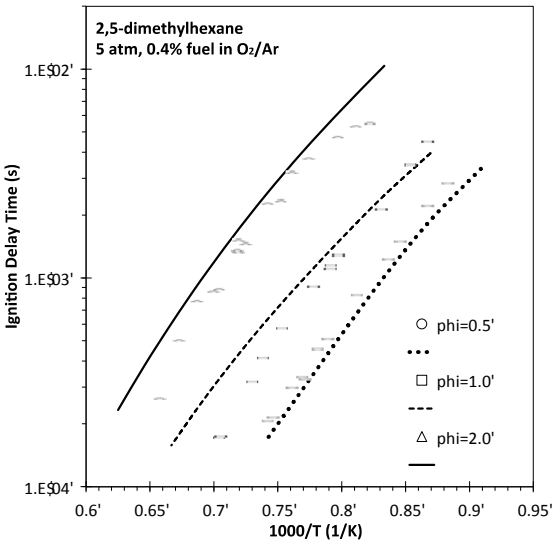

Figure 7 – ST ignition delay measurements (symbols) and model predictions (lines) for 0.4% 2,5-dimethylhexane in O_2/Ar mixture at 5 atm and three equivalence ratios.

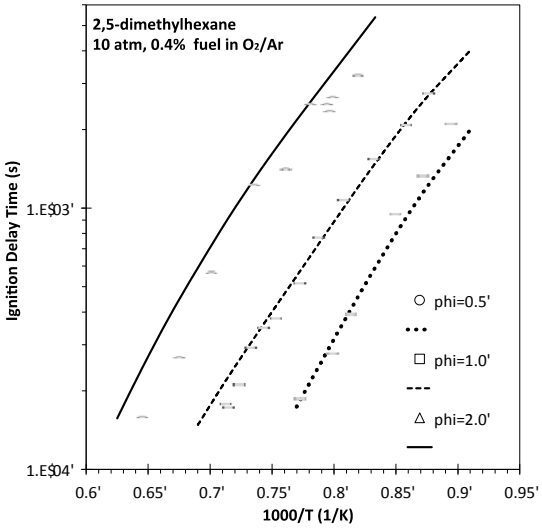

Figure 8 – ST ignition delay measurements (symbols) and model predictions (lines) for 0.4% 2,5-dimethylhexane in O_2/Ar mixture at 10 atm and three equivalence ratios.

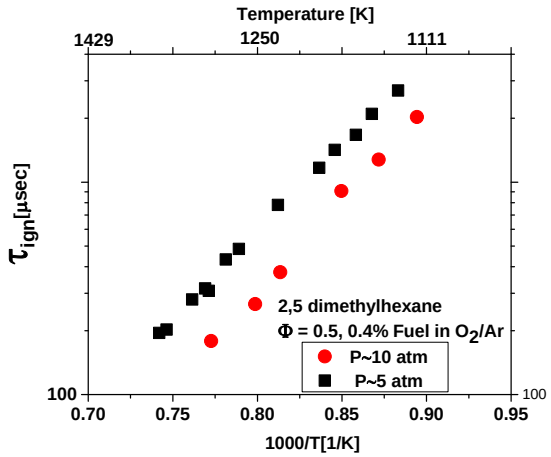

Figure 9 – Effect of pressure on the measured ST ignition delay times for 2,5-dimethylhexane at Φ = 0.5

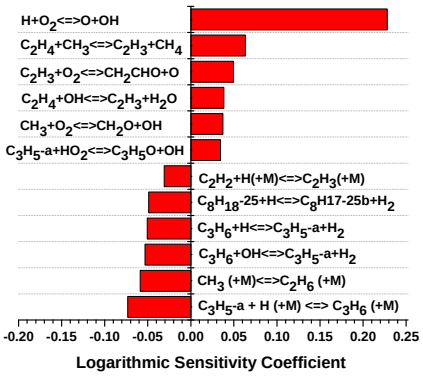

Figure 10 –Ranked logarithmic Temperature A-factor sensitivity coefficients at the time of ignition for 0.4% 2,5-dimethylhexane in O_2/Ar mixture at 10 atm, φ =1, and temperature of 1470K.

Shock tube ignition measurements in air

Kinetic modeling simulations are compared to the Rensselaer shock tube measurements for 2,5-dimethylhexane/air ignition delay times in **Figure 11** (20 atm) and **Figure 12** (40 atm). Equivalence ratios of 0.5, 1 and 2 were considered by varying the fuel concentration. Simulations were carried out using the adiabatic homogenous reactor model in CHEMKIN PRO [42] with an imposed volume history to account for the experimentally measured pressure gradient, $dP/dt(1/P_0)$ = 3% ms^{-1}, due to viscous gasdynamics.

The shock tube measurements show three distinct regions of reactivity. In both experiments at temperatures greater than ~850 K, the ignition delay time decreases with increasing temperature. In an intermediate temperature window from around 750 to 850 K, the ~20 atm shock tube results show mild NTC behavior in some cases and indiscernible temperature dependence in others, exhibited by a plateau in ignition delay. At temperatures below around 750 K ignition delay

begins to increase with decreasing temperature again, particularly evident in the $\varphi = 2$ case. The kinetic modeling also illustrates the three regions of reactivity but predicts transition temperatures from high-temperature to NTC behavior for the three equivalence ratios studied that are slightly greater than those measured. The NTC behavior is well predicted by the model. Overall, the kinetic model does predict well the ignition delay times in the NTC region and the high-temperature apparent activation energy. The present model predicts ignition delay times above ~950 K at both 20 atm and 40 atm better than previous model presented for other octane isomers [16,20]. This is attributed to the increased rate constant employed for hydrogen abstraction by HO_2 radicals, since reactivity is controlled to a large extent by fuel + HO_2 → radical + H_2O_2 followed by $H_2O_2 + M \rightarrow 2OH + M$. In the NTC and low-temperature regions ($T < 850$ K) the kinetic modeling predictions are within a factor of 1.5 of shock tube ignition delay time measurements but in many specific cases the experiment-model agreement is much better, with differences of only tens of percents.

The crossover in equivalence ratio dependence observed in the modeling predictions at the highest temperatures (~1250 K in **Figure 11** and **Figure 12**) is the result of the temperature dependence of the competition between $H + O_2 \rightarrow OH + O$ and $H + O_2 + M \rightarrow HO_2 + M$. For $T <$ 1250 K at the elevated pressures (20 and 40 atm), $H + O_2 + M \rightarrow HO_2 + M$ dominates and the HO_2 formed in this reaction largely goes on to abstract an H atom from 2,5-dimethylhexane to yield hydrogen peroxide which subsequently decomposes to form two OH radicals, providing radical branching the rate of which increases with increasing 2,5-dimethylhexane concentration. In these experiments with fuel/air mixtures, the fuel concentration increases with equivalence ratio. Therefore, at $T < 1250$ K and elevated pressures, increasing the equivalence ratio results in increased radical branching and decreased ignition delay. For $T > 1250$ K, $H + O_2 \rightarrow OH + O$ dominates and increasing the 2,5-dimethylhexane concentration increases the rate of H atom scavenging by 2,5-dimethylhexane and reduces the net radical branching rate. Hence, increasing the equivalence ratio at these higher temperatures, results in increased ignition delay. While the experiments do not show the crossover in equivalence ratio dependence, they do exhibit decreased influence of equivalence ratio for increasing temperature.

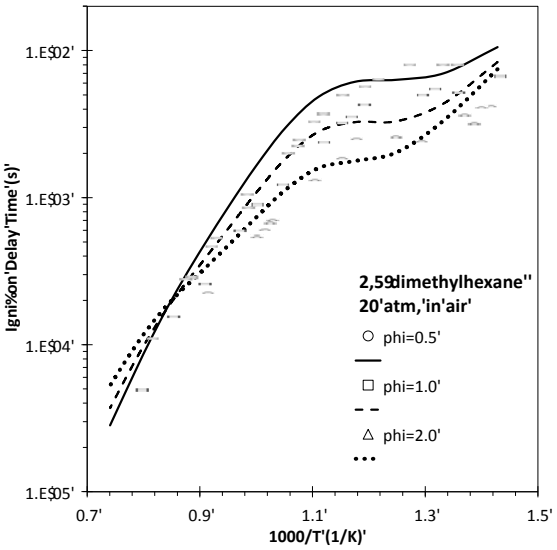

Figure 11 – ST ignition delay measurements (symbols) and model predictions (lines) for 2,5-dimethylhexane in air near 20 atm and three equivalence ratios.

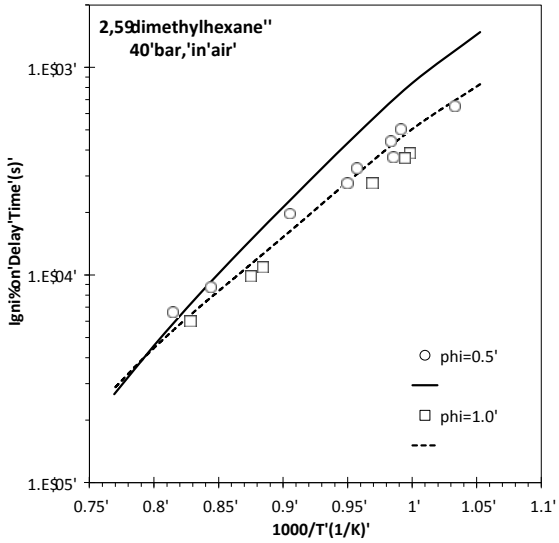

Figure 12 - ST ignition delay measurements (symbols) and model predictions (lines) for 2,5-dimethylhexane in air near 40 atm and three equivalence ratios.

A temperature A-factor sensitivity analysis at the time ignition for 20 atm, 950 K, and three equivalence ratios is shown in **Figure 13**. A positive sensitivity coefficient indicates that increasing the reaction rate constant will increase reactivity and hence decrease ignition delay times. The decomposition of H_2O_2 to two OH radicals is the most sensitive reaction at these conditions, and hydrogen abstraction by HO_2 from the tertiary site also exhibits a strong sensitivity since it produces H_2O_2 while depleting the fuel. The recombination of two HO_2 radicals to form H_2O_2 and O_2 exhibits a negative sensitivity, as this competes with the hydrogen abstraction channel. The oxidation of 2,5-deimthylhexane leads to the production of iso-butene, propene, and methyl radicals, so reactions involving these species also appear in the sensitivity analysis. The decomposition of the fuel-derived alkenyl radical (C_8H_{15}-1-25) is presented as

important in the sensitivity analysis. This radical is a "lumped" species in the kinetic model representing the various alkenyl radicals formed followed hydrogen abstraction from one of the three 2,5-dimethylhexene isomers. These alkenes are formed in the NTC region via concerted elimination of HO_2 from alkylperoxy radicals (RO2 → HO2 + alkene). The sensitivity analysis indicates that improving the fidelity of the alkene sub-mechanism, such as done by Mehl et al. for hexene isomers [43], would impact the model's ignition delay time predictions at 950 K.

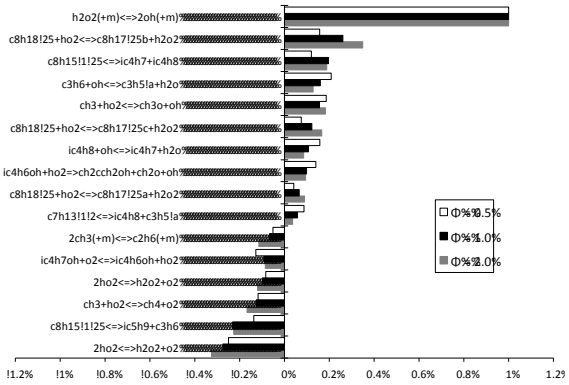

Figure 13 - Temperature A-factor sensitivity coefficients at the time of ignition for 2,5-dimethylhexane in in air near 20 atm, φ =1, and temperature of 950 K.

Reactivity of octane isomers under ST conditions

The shock tube ignition delay data in air at 20 atm presented here for 2,5-dimethylhexane allows comparison of reactivity with other octane isomers (e.g., n-octane, 2-methylheptane, and 3-methylheptane) for which data has been obtained previously [16,20]. The measured reactivity of the various octane isomers is similar at temperatures above 900 K, but differences are observed in the NTC region. Mehl et al. [44,45] have proposed that the ignition quality of a gasoline fuel, quantified as antiknock index, can be closely correlated with its ST ignition delay time under specific conditions (e.g., 825 K and 25 atm). **Figure 14** demonstrates that such a correlation exists for various octane isomers using experimental and simulated ignition delay times near 20 atm and 835 K. The logarithm of experimental shock tube ignition delay data for n-octane, 2-methylheptane, 3-methylheptane, and 2,5-dimethylhexane increases as the RON of the fuel increases. Simulations of ignition delay well reproduce this correlation, and further demonstrate that it can be extrapolated to iso-octane (2,2,4-trimethylpentane) for which experimental data is not available.

In the NTC and low-temperature regions, where differences in ignition delay are observed and predicted for the four C_8 isomers, the reactivity is controlled by competition between the low-temperature chain branching pathway (R + O_2 ↔ RO_2 ↔ QOOH (+O_2) ↔ O_2QOOH → 2OH + R + stable) and inhibitive pathways including the concerted elimination of HO_2 from alkylperoxy radicals (RO2 → HO_2 + alkene), the formation of cyclic ethers from hydroperoxyalkyl radicals (QOOH → cyclic ether + OH), and the beta scission of hydroperoxylalkyl radicals (QOOH → R + beta-scission products). Sarathy et al. [20] have shown that the differences in NTC and low-temperature reactivity between n-octane and 2-methylheptane is due to the different C-H bond

strengths in the molecules and their effect on the rates of isomerization reactions (H-atom transfer reactions) in the low-temperature chain branching sequence that leads to ketohydroperoxide species. The decreased reactivity of 2,5-dimethylhexane compared to 2-methylheptane can be attributed to the presence of an additional tertiary site (two in total), which further inhibits low temperature chain branching pathways.

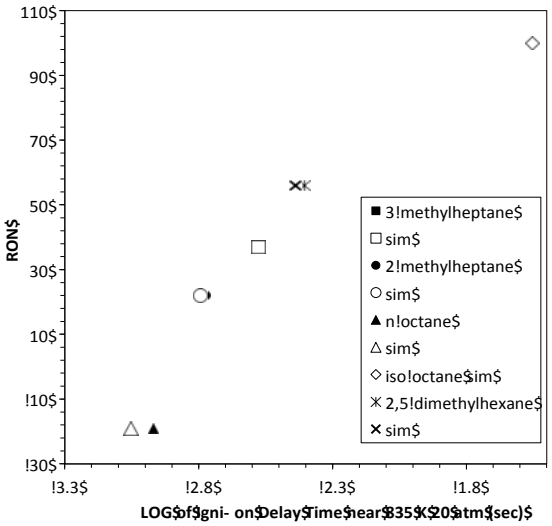

Figure 14 – Correlation of research octane number (RON) with logarithm of ignition delay time near 835 K and 20 atm (ST measurements – solid symbols, simulations – open symbols).

Rapid compression machine ignition

The experimental and kinetic modeling results for 2,5-dimethylhexane under RCM conditions of 5 and 10 atm and three equivalence ratios (0.5, 1.0, and 2.0) are shown in **Figure 15**, **Figure 16**, and **Figure 17**. The experimental data under RCM conditions exhibit similar trends as those observed earlier under ST experiments at 20 atm, wherein a decrease in ignition delay times with increased temperature is observed at low temperatures (LT region), followed by NTC behavior at intermediate temperatures (NTC region), and finally Arrhenius temperatures dependence above 900 K (HT region). Kinetic modeling predictions using constant volume simulations appear to be in good qualitative agreement with the experimental data in predicting the transitions from low temperature Arrhenius behavior to intermediate temperature NTC behavior and then to high temperature Arrhenius behavior. At $\varphi = 0.5$, the model simulations utilizing the experimentally derived volume histories well predict the experimental data acquired at 5 atm, while the 10 atm data is predicted to within a factor of 2.

The most significant discrepancies between predicted and measured RCM ignition delays are at $\varphi = 1.0$ and $\varphi = 2.0$, as shown in **Figure 16** and **Figure 17**. At 10 atm, the constant volume model ignition delay time predictions in the LT region are consistently longer than the experimental measurements at both at $\varphi = 1.0$ and $\varphi = 2.0$. Simulations employing volume histories to account for experimental heat loss worsen the prediction, as these further increase ignition times. An attempt was made to increase low temperature reactivity of the kinetic model

by reducing the activation energy of ketohydroperoxide decomposition by 7 kcal/mol (from 39 kcal/mol to 32 kcal/mol); however, this modification could not resolve the discrepancy between model predictions and experiments. A sensitivity analysis presented in **Figure 18** indicates that the recombination of two HO_2 radicals to form H_2O_2 and O_2 exhibits a negative sensitivity that becomes increasingly important at richer conditions. This suggests that decreasing this rate constant would decrease ignition delay times at stoichiometric and rich conditions, while not degrading the model's already acceptable prediction at lean conditions.

Figure 16 (φ = 1.0) and **Figure 17** (φ = 2.0) also show that the kinetic model under predicts measured ignition delay times in the NTC region under constant volume conditions at 5 atm and 10 atm. Thus, the constant volume model is too reactive in the NTC region. Simulations employing volume histories to account for heat losses are expected to improve agreement between the model and experiments; however, the decrease in reactivity is not sufficient to reconcile the disagreement. The dependence of the ignition delay time on temperature is weaker within the NTC regime, so the effect of the non-constant volume conditions is not as strong. The presence of the RCM crevice region could eventually influence the NTC behavior when multi-stage ignition occurs. The pressure rise due to the first stage ignition is reduced in experiments since a mass flow from the combustion chamber into the crevice occurs [46,47]. This effect should be quite small, but a worst-case estimation is made by forcing the simulation to follow a non-reactive pressure profile that completely suppresses the pressure increase due to first stage ignition. This represents a crevice with infinite volume. The results of the "pressure history" simulations shown in **Figure 16** and **Figure 17** indicate a notable decrease in the model's reactivity and an improved agreement with the experimental data in the NTC region.

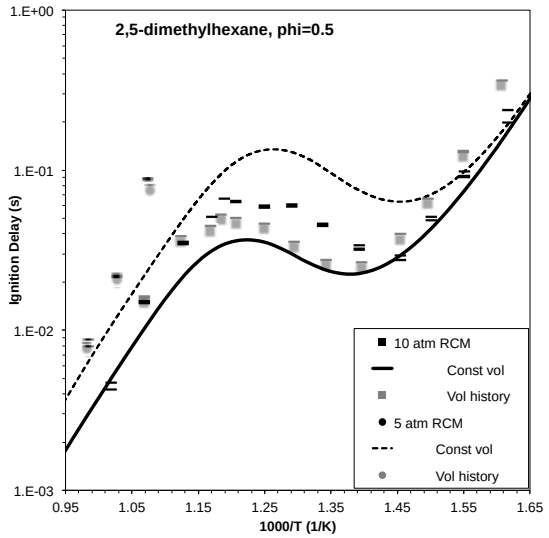

Figure 15 - RCM ignition delay measurements (symbols) and model predictions (lines – constant volume, gray symbols – volume history) for 2,5-dimethylhexane in air at φ =0.5 and pressures of 5 atm and 10 atm.

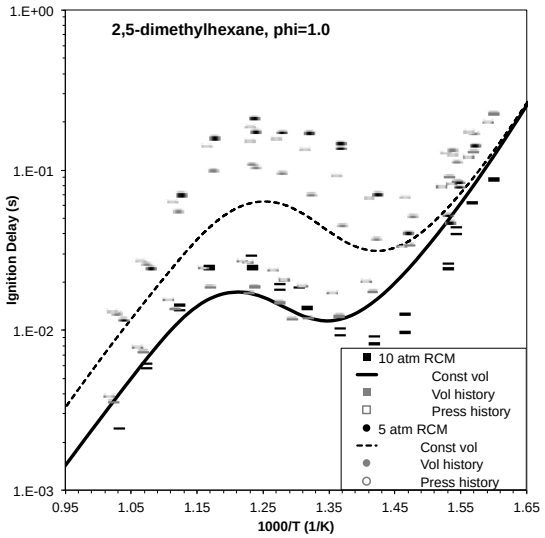

Figure 16 - RCM ignition delay measurements (symbols) and model predictions (lines – constant volume, solid gray symbols – volume history, open gray symbols – pressure history) for 2,5-dimethylhexane in air at φ =1.0 and pressures of 5 atm and 10 atm.

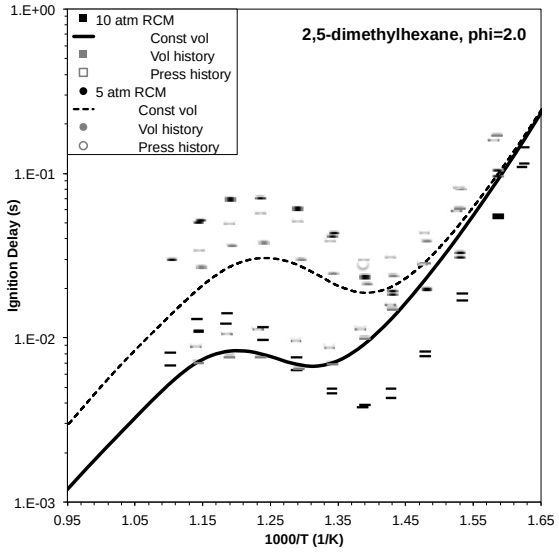

Figure 17 - RCM ignition delay measurements (symbols) and model predictions (lines – constant volume, solid gray symbols – volume history, open gray symbols – pressure history) for 2,5-dimethylhexane in air at φ =2.0 and pressures of 5 atm and 10 atm.

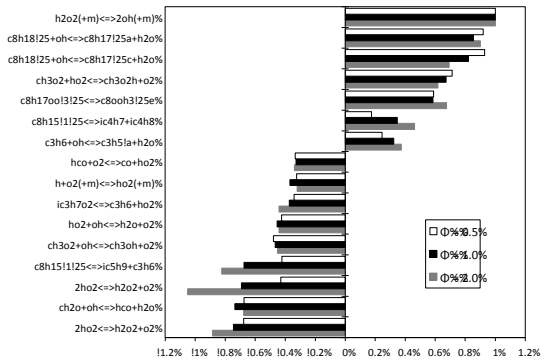

Figure 18 - Temperature A-factor sensitivity coefficients at the time of ignition for 2,5-dimethylhexane in in air near 10 atm, φ =1, and temperature of 650 K.

Figure 19 presents a reaction path analysis for 2,5-dimethylhexane ignition delay at 650 K, 10 atm, φ =1.0, and 20% of the fuel consumed. At these low temperature conditions, the fuel is consumed primarily by hydrogen abstraction by OH radicals from the primary, secondary, and tertiary sites. The fuel radicals then react with molecular oxygen to form alkylperoxy (RO_2) radicals, which primarily isomerize to form QOOH radicals. The fate of the secondary fuel radical is presented in more detail, as this one contributes most to the system's low temperature reactivity. The secondary RO_2 radical undergoes a rapid internal H-atom migration via a 6-membered ring transition state with the tertiary site to form a QOOH radical. This radical reacts with molecular oxygen to form O_2QOOH that isomerizes to form a ketohydroperoxide plus OH radical. The ketohydroperoxide eventually decomposes to smaller oxygenates and OH radical, thus completing the low temperature chain branching sequence.

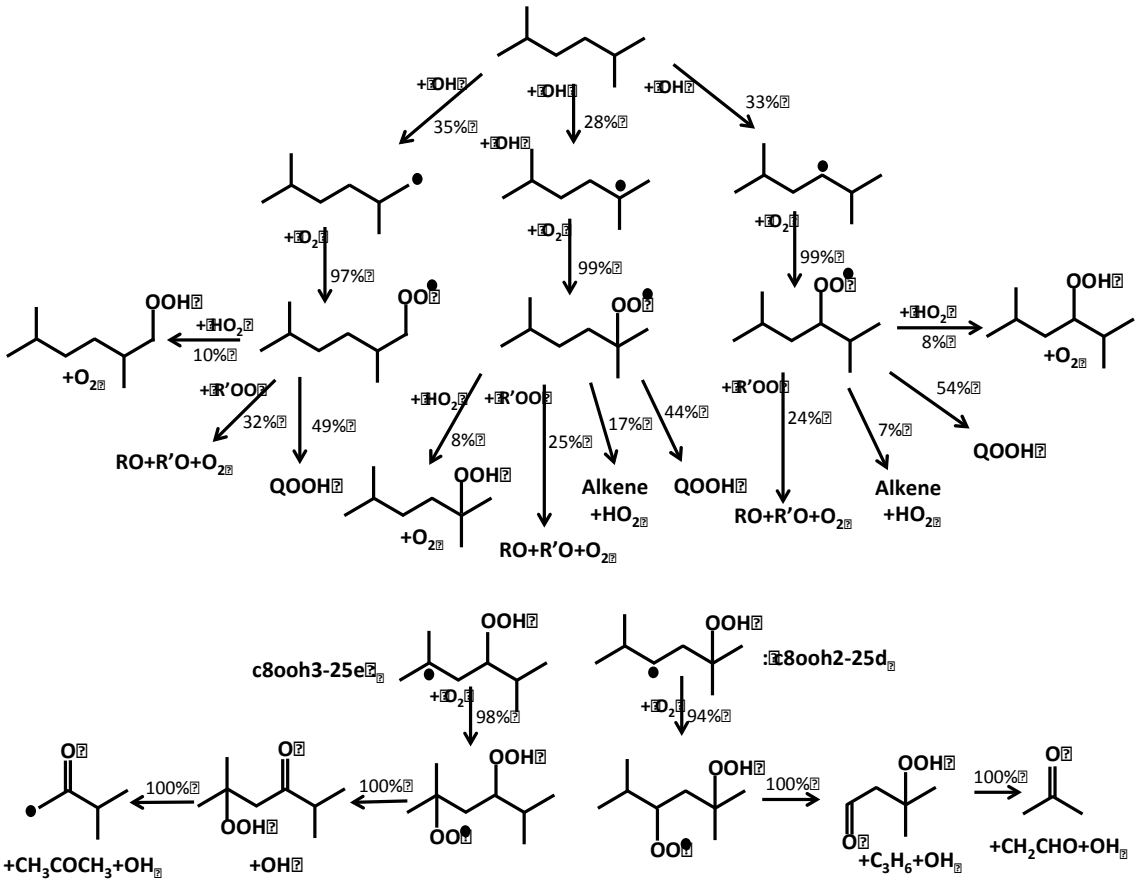

Figure 19 - Reaction path analysis for 2,5-dimethylhexane at 650 K, 10 atm, φ =1.0. The reaction fluxes are given for 20% fuel consumption

Jet stirred reactor oxidation

The jet stirred reactor is a fundamental experimental tool for understanding the low temperature and high temperature reactivity, as well as the major and minor species formed at various temperatures and equivalence ratios. The experiments presented herein were conducted at high pressure (i.e., 10 atm) to better study the low temperature reactivity under conditions similar those found in internal combustion engines. The JSR experimental setup utilized in previous studies on 2-methylheptane and 2-methylheptane was employed here to generate data for 2,5-dimethylhexane. This allowed a direct comparison between the results obtained here those obtained previously under the same conditions with the mono-methylated heptanes (Table 1).The structure of the octane fuel isomer (2,5-dimethylhexame, 3-, or 2-methylheptane) has strong impact on the type and amount of intermediate products formed.. The production of 2-butene and 2-methyl-1-butene is observed in 3-methylheptane experiments, whereas these products were not reported for 2,5-dimethylhexane and 2-methylheptane under identical conditions. iso-Butene and propene are measured in greatest concentrations in 2,5-dimethylhexane due to the two methyl branches facilitating formation of these compounds following hydrogen abstraction and beta scission reactions [13]. Acetone is primarily formed from iso-butene, hence its increased concentration in the 2,5-dimethylhexane experiments. 2-methyl-1-butene was detected in the 3-

methylheptane experiments, but not in the 2,5-dimethylhexane or 2-methylheptane experiments. Instead, the pentene isomer 3-methyl-1-butene was measured in significant amounts during the oxidation of 2,5-dimethylhexane and 2-methylheptane. In summary, the species measured at greater amounts during oxidation of 2,5-dimethylhexane can be attributed directly to is highly branched structure and the high temperature reaction pathways discussed in [13].

Table 1. Maximum mole fractions in ppm of intermediates measured during the oxidation of 2,5-dimethylhexane, 3-, and 2-methylheptane in a JSR at 10 atm, φ =1, 0.7s and 800-1200 K.

Species	2,5-dimethylhexane	3-methylheptane	2-methylheptane
CO	4540	4460	3740
CH_2O	247	262	257
CH_3CHO	60	99	74
2-propenal	30	41	31
Acetone	203	33	86
CH_4	671	588	432
C_2H_4	523	1080	852
C_3H_6	425	282	300
1-C_4H_8	15	93	36
2- C_4H_8	< 5	49	< 4
Iso-C_4H_8	174	13	77
1,3-butadiene	10	21	15
2-methyl-1-butene	N/A	62	< 3
2-methyl-3-butene	77	N/A	121

The CHEMKIN PRO [42] transient perfectly stirred reactor code was used to validate the proposed kinetic model against jet stirred reactor data for 2,5-dimethylhexane at 10 atm, three equivalence ratios (φ = 0.5, φ = 1.0, and φ = 2.0), and a range of temperatures between 500-1200 K. The fuel was kept constant at 0.1% and the O_2 concentration was changed to vary equivalence ratio. The important measured species are the fuel 2,5-dimethylhexane (C_8H_{16}-25), hydrogen (H_2), oxygen (O_2), water (H_2O), carbon monoxide (CO), carbon dioxide (CO_2), methane (CH_4), acetylene (C_2H_2), ethylene (C_2H_4), propene (C_3H_6), ethanal (CH_3CHO), formaldehyde (CH_2O), 2-methylpropanal (iC_3H_7CHO), acetone (CH_3COCH_3), *2*-propenal (C_2H_3CHO), *1*-butene (1-C_4H_8), *iso*-butene (iC_4H_8), *1,3*-butadiene (1,3-C_4H_6), 2-methyl-3-butene (C_5H_{10}-3-2), 2-methyl-1-hexene (C_8H_{16}-1-25), 2-methyl-2-hexene (C_8H_{16}-2-25), and 2,2,5,5-tetramethyl-tetrahydrofuran ($C_8H_{16}O_2$-5-25).

Figure 20 presents the experimental measurements and modeling results of 2,5-dimethylhexane obtained at φ =1.0. The experimental results (symbols) show that with increasing temperature, the 2,5-dimethylhexane concentration drops significantly between 500 K and 650 K. This corresponds to the cool flame reactivity regime, wherein the overall low temperature peroxy radical sequence is active leading to chain branching. In this region, the first maximum of several oxygenated compounds (e.g., formaldehyde, acetone, 2-methylpropanal, and ethanal) is created

from the decomposition of ketohydroperoxide species. From 650 K to 750 K, there is an increase in the 2,5-dimethylhexane concentrations exhibiting the NTC behavior of the system, wherein reactions involving dissociation of RO_2 back to $R+O_2$, concerted elimination of HO_2, and cyclic ether formation become important. Many alkene species reach their maximum concentration around 850 K and are then destroyed at higher temperature. 850 K also corresponds to a second maximum in the concentration of small oxygenates.

The model predictions for φ =1.0 are also shown in **Figure 20**, whereas **Figure 21** and **Figure 22** present the results at other equivalence ratios. The model's ability to reproduce the experimental data is discussed qualitatively and quantitatively. The model's prediction is considered good if the shape of the model profile closely matches the experimental profile, and if the predicted maximum mole fraction is within a factor 2 of the measured maximum mole fraction. The concentration of the reactants of 2,5-dimethylhexane and O_2 is well predicted at the lowest and highest temperatures, and so is the concentration of the major product species CO, CO_2, and H_2O. Similarly the model and experiments agree in the NTC region, wherein the model is able to capture the decrease in reactivity from 700 to 750 K. The model is able to capture the double peaks of both 2-methyl-1-hexene (C_8H_{16}-1-25) and 2-methyl-2-hexene (C_8H_{16}-2-25) in the NTC region. At temperatures above 850 K, there is an under prediction of C_2H_4 and CH_4 profiles, but these predictions improve at richer conditions.

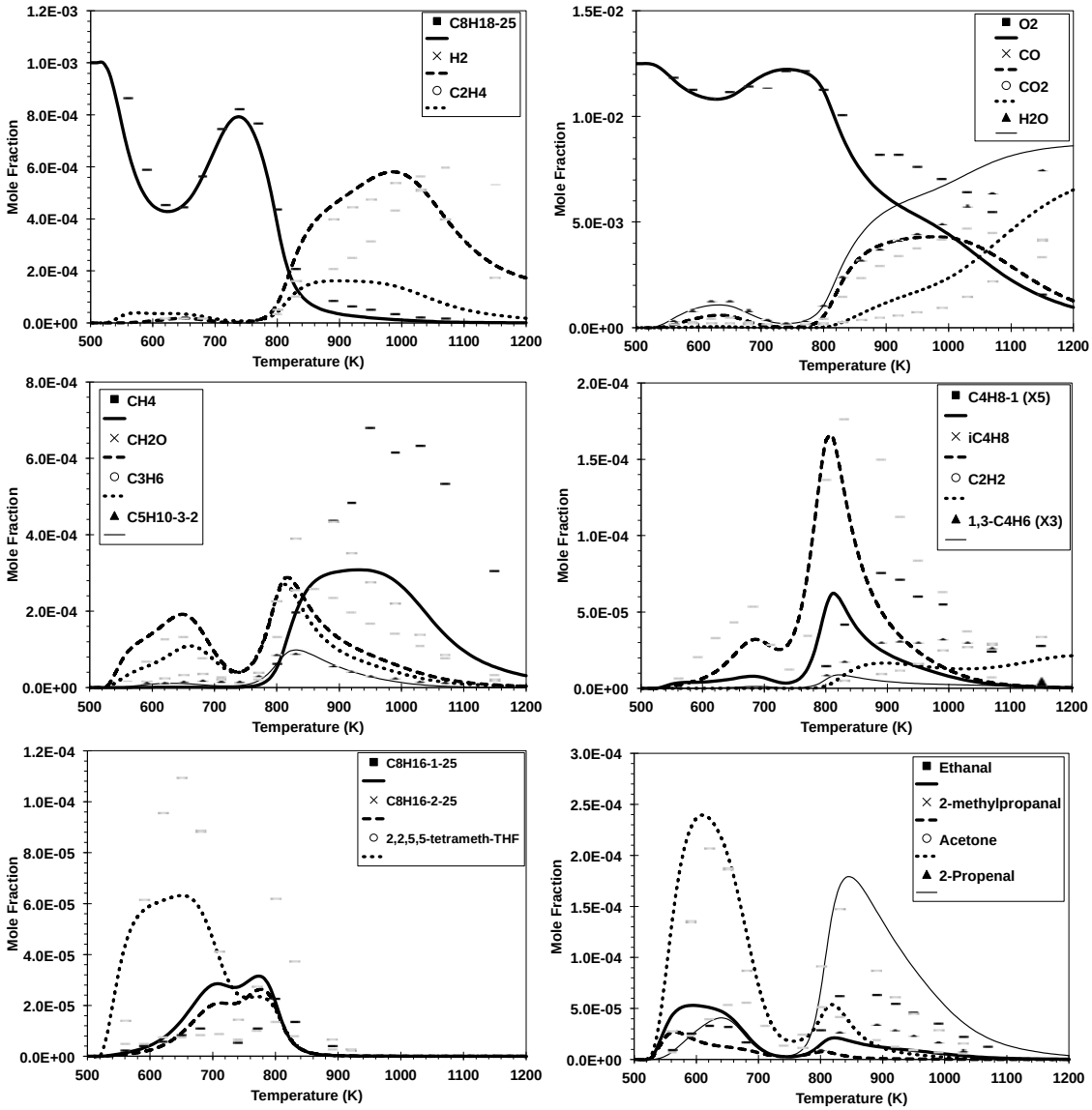

Figure 20 - Species mole fraction profiles for 2,5-dimethylhexane oxidation versus reactor temperature in a JSR at 10 atm, τ = 0.7 s and φ = 1.0. The initial fuel (C8H18-25) mole fraction was 0.1%. Experimental data (symbols) are compared to calculations (lines).

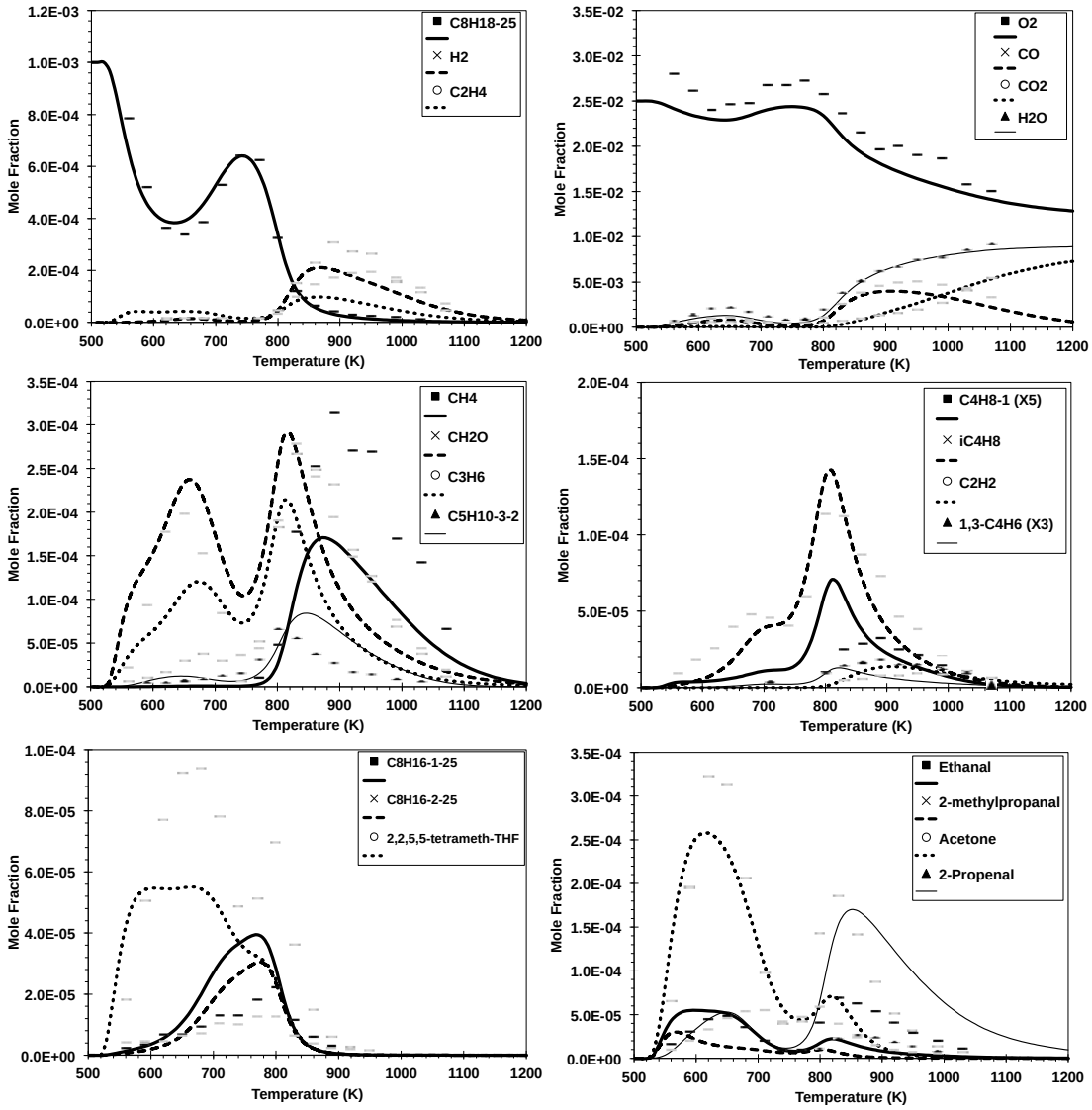

Figure 21 - Species mole fraction profiles for 2,5-dimethylhexane oxidation versus reactor temperature in a JSR at 10 atm, τ = 0.7 s and φ = 0.5. The initial fuel (C8H18-25) mole fraction was 0.1%. Experimental data (symbols) are compared to calculations (lines).

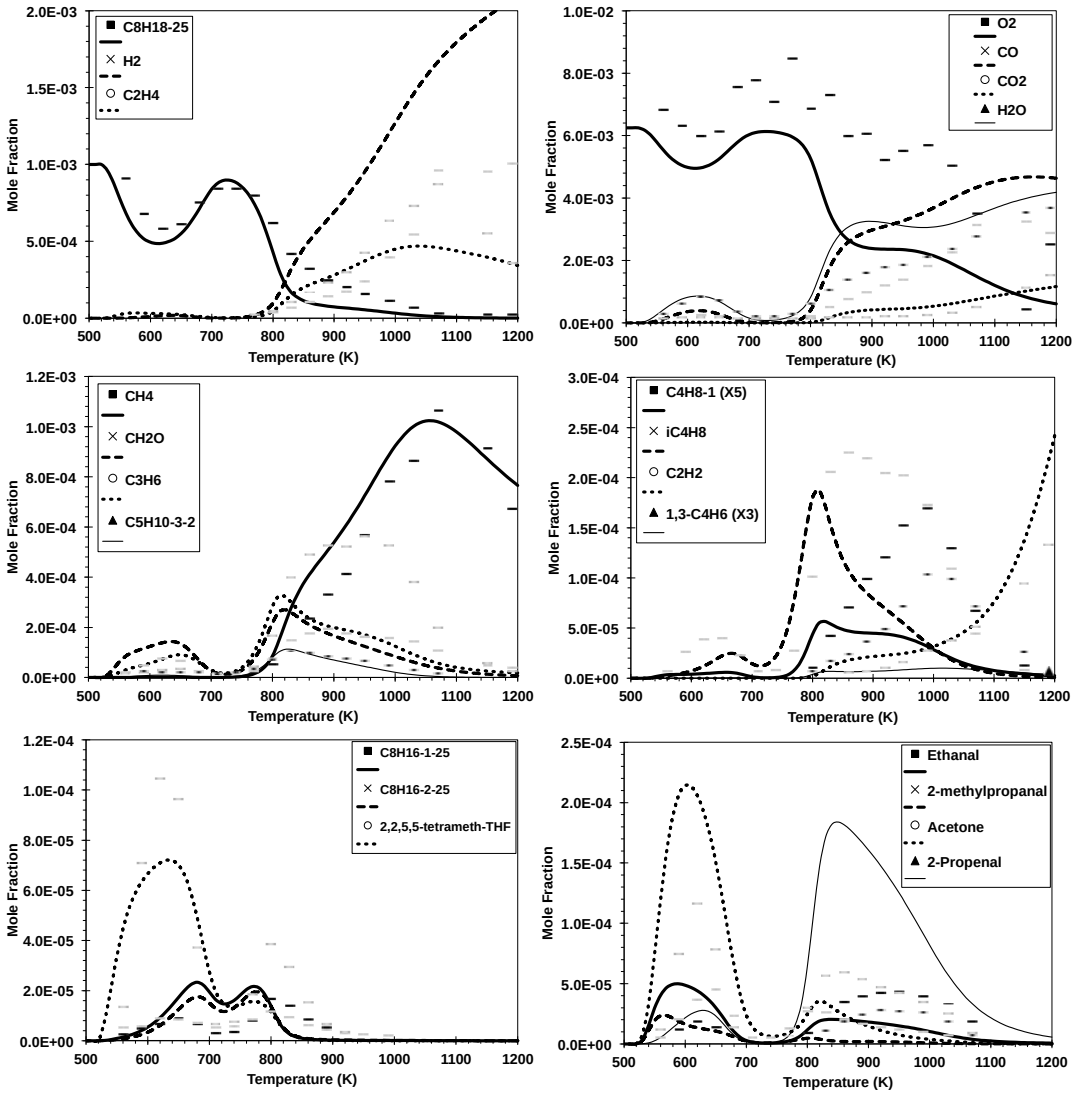

Figure 22 - Species mole fraction profiles for 2,5-dimethylhexane oxidation versus reactor temperature in a JSR at 10 atm, τ = 0.7 s and φ = 2.0. The initial fuel (C8H18-25) mole fraction was 0.1%. Experimental data (symbols) are compared to calculations (lines).

Reaction path analyses are presented for 2,5-dimethylhexane in a JSR at 10 atm, three equivalence ratios, and temperatures of 650 K (**Figure 23**) and 800 K (**Figure 24**). At 650 K, the reactions responsible for consuming the fuel in the fixed residence time JSR are consistent with those presented at 600 for ignition in a transient constant volume batch reactor. The fuel reactivity is driven by the initial abstraction of hydrogen from the fuel followed by conventional low temperature chain branching via R + O_2 ↔ RO_2 ↔ QOOH (+O_2) ↔ O_2QOOH → 2OH + R + stable. At 800 K, pathways inhibiting reactivity become important, such as alkyl radical decomposition (beta scission) and concerted elimination of HO_2 from alkylperoxy radicals (RO2 → HO2 + alkene). Also, alkyl isomerization of the 25-dimethyl-1-hexyl radical has a significant role and leads to the formation of iso-butene (iC_4H_8).

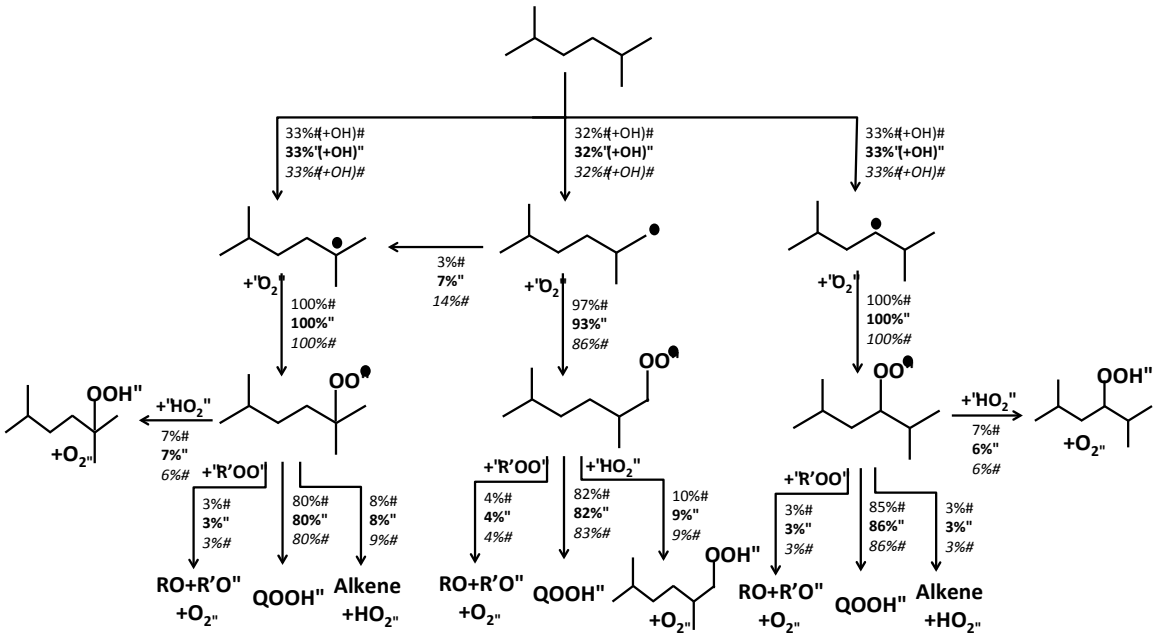

Figure 23 – Reaction path analysis for 2,5-dimethylhexane in a JSR at 10 atm, 600 K, τ = 0.7 s and three equivalence ratios. Plain text φ =0.5, bold text φ =1.0, italicized text φ =2. The initial fuel (C8H18-25) mole fraction was 0.1%.

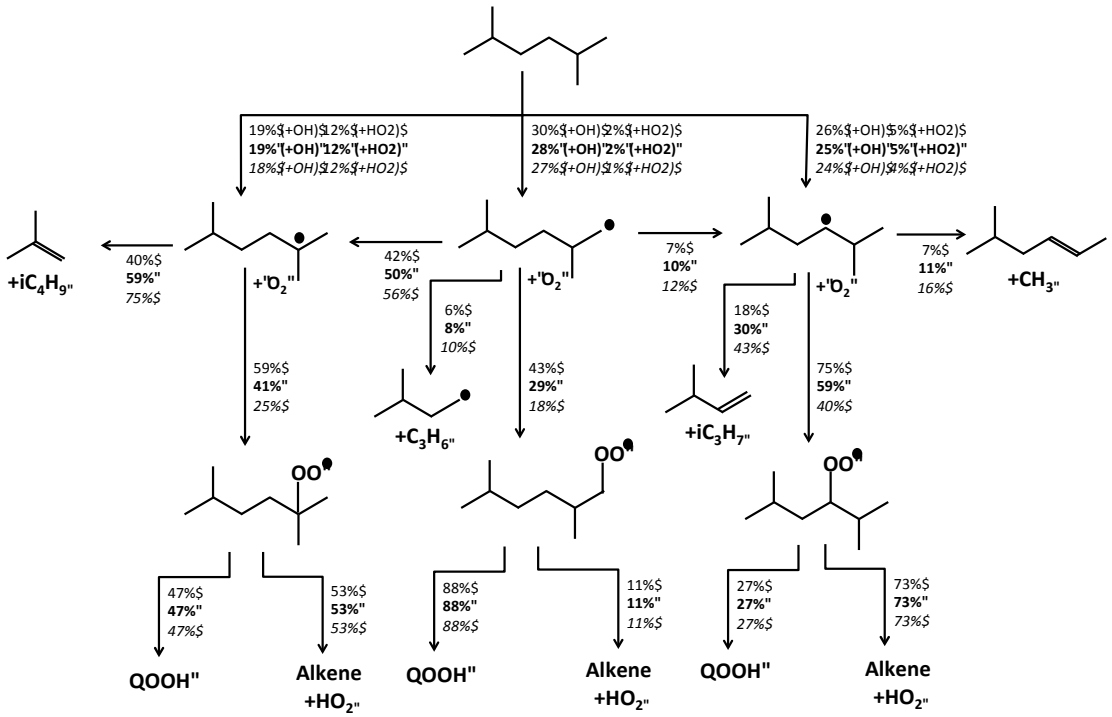

Figure 24 - Reaction path analysis for 2,5-dimethylhexane in a JSR at 10 atm, 800 K, τ = 0.7 s and three equivalence ratios. Plain text φ =0.5, bold text φ =1.0, italicized text φ =2. The initial fuel (C8H18-25) mole fraction was 0.1%.

Conclusions – All

A comprehensive experimental and kinetic modeling study of the oxidation of 2,5-dimethylhexane has been carried out. The newly developed detailed kinetic model for 2,5-dimethylhexane shows generally good agreement with ignition delay measurements from shock tubes and a rapid compression machine and speciation measurements from a jet-stirred reactor.

Comparisons of shock tube ignition delay time measurements carried out at high temperatures with kinetic modeling predictions highlight the importance of propene chemistry, as propene is formed in large quantities from 2,5-dimethylhexane decomposition. At intermediate temperatures (~900-1000 K), HO_2 and H_2O_2 chemistry is highly sensitive, as is the abstraction of H atoms from 2,5-dimethylhexane by HO_2 to produce H_2O_2. There is a need for more accurate rate constants for reactions involving HO_2 including its reaction with 2,5-dimethylhexane and with allyl radical. At temperatures less than ~850 K, the competition between the conventional low-temperature radical branching sequence and inhibitive propagation pathways controls reactivity and it is shown that the logarithm of the ignition delay time for four octane isomers (n-octane, 2-methylheptane, 3-methylheptane, and 2,5-dimethylhexane) correlates well with the Research Octane Number (RON).

Comparisons of simulated and experimental results highlighted the need for more accurate rate constants for the reaction of HO_2 with the fuel and with propene.

Please add your comments here

Acknowledgments - All
All please add your acknowledgements here

The work at KAUST was funded by the Clean Combustion Research Center and by Saudi Aramco under the FUELCOM program. The Rensselaer group was supported by the U.S. Air Force Office of Scientific Research (Grant No. FA9550-11-1-0261) with Dr. Chiping Li as technical monitor. The LLNL work was performed under the auspices of the US Department of Energy by Lawrence Livermore National Laboratory under Contract DE-AC52-07NA27344 and was supported by the US Department of Energy, Office of Vehicle Technologies. At CNRS, the research leading to these results has received funding from the European Research Council under the European Community's Seventh Framework Programme (FP7/2007-2013) / ERC grant agreement n° 291049 − 2G-CSafe.

References

[1] K. Schofield, Energy Fuels 26 (2012) 5468-5480.
[2] W.J. Pitz, C.J. Mueller, Prog. Energy Combust. Sci. 37(2011) 330-350.
[3] M. Serve, D. Bombick, J. Roberts, G. McDonald, Chemosphere 22 (1991) 77-84.
[4] M. Alnajjar, B. Cannella, H. Dettman, C. Fairbridge, J. Franz, T. Gallant, R. Gieleciak, D. Hager, C. Lay, S. Lewis, Coordinating Research Council Technical Report (2010).
[5] J. Smith, J. Simmie, H. Curran, Int. J. Chem. Kinet. 37 (2005) 728-736.
[6] D. Smith, K. Ledingham, H. Kilic, T. McCanny, W. Peng, R. Singhal, A. Langley, P. Taday, C. Kosmidis, J. Phys. Chem. A 102 (1998) 2519-2526.
[7] G. Knothe, Prog. Energy Combust. Sci.36 (2010) 364-373.
[8] T.J. Bruno, E. Baibourine, Energy Fuels 25 (2011) 1847-1858.
[9] T. Bruno, E. Baibourine, Energy Fuels 24 (2010) 5508-5513.
[10] M.L. Huber, B.L. Smith, L.S. Ott, T.J. Bruno, Energy Fuels 22 (2008) 1104-1114.
[11] F. Karsenty, S.M. Sarathy, C. Togbé, C.K. Westbrook, G. Dayma, P. Dagaut, M. Mehl, W.J. Pitz, Energy Fuels 26 (2012) 4680-4689.
[12] S. Sarathy, C. Yeung, C. Westbrook, W. Pitz, M. Mehl, M. Thomson, Combust. Flame 158 (2011) 1277-1287.
[13] S. Mani Sarathy, U. Niemann, C. Yeung, R. Gehmlich, C.K. Westbrook, M. Plomer, Z. Luo, M. Mehl, W.J. Pitz, K. Seshadri, Proc. Combust. Inst. 34 (2013) 1015-1023.
[14] N. Liu, S.M. Sarathy, C.K. Westbrook, F.N. Egolfopoulos, Proc. Combust. Inst. 34 (2013) 903-910.
[15] C. Ji, S.M. Sarathy, P.S. Veloo, C.K. Westbrook, F.N. Egolfopoulos, Combust. Flame 159 (2012) 1426-1436.
[16] W. Wang, Z. Li, M.A. Oehlschlaeger, D. Healy, H.J. Curran, S.M. Sarathy, M. Mehl, W.J. Pitz, C.K. Westbrook, Proc. Combust. Inst. 34 (2013) 335-343.
[17] S. Dooley, S.H. Won, S. Jahangirian, Y. Ju, F.L. Dryer, H. Wang, M.A. Oehlschlaeger, Combust. Flame 159 (2012) 1444-1466.
[18] C.J. Mueller, W.J. Cannella, T.J. Bruno, B. Bunting, H.D. Dettman, J.A. Franz, M.L. Huber, M. Natarajan, W.J. Pitz, M.A. Ratcliff, K. Wright, Energy Fuels 26 (2012) 3284-

3303.
[19] C. Allen, D. Valco, E. Toulson, T. Edwards, T. Lee, Combust. Flame 160 (2013) 232-239.
[20] S.M. Sarathy, C.K. Westbrook, M. Mehl, W.J. Pitz, C. Togbé, P. Dagaut, H. Wang, M.A. Oehlschlaeger, U. Niemann, K. Seshadri, P.S. Veloo, C. Ji, F.N. Egolfopoulos, T. Lu, Combust. Flame 158 (2011) 2338-2357.
[21] E. Silke, H. Curran, J. Simmie, Proc. Combust. Inst. 30 (2005) 2639-2647.
[22] C. Westbrook, W. Pitz, H. Curran, J. Boercker, E. Kunrath, Int. J. Chem. Kinet. 33 (2001) 868-877.
[23] C. Westbrook, W. Pitz, J. Boercker, H. Curran, J. Griffiths, C. Mohamed, M. Ribaucour, Proc. Combust. Inst. 29 (2002) 1311-1318.
[24] C. Morley, Combust. Sci. Technol. 55 (1987) 115-123.
[25] W.K. Metcalfe, S.M. Burke, S.S. Ahmed, H.J. Curran, International Journal of Chemical Kinetics (2013) doi:10.1002/kin.20802.
[26] H. Curran, P. Gaffuri, W. Pitz, C. Westbrook, Combust. Flame 129 (2002) 253-280.
[27] J. Aguilera-Iparraguirre, H. Curran, W. Klopper, J. Simmie, J. Phys. Chem. A 112 (2008) 7047-7054.
[28] H.-H. Carstensen, A.M. Dean, O. Deutschmann, Proc. Combust. Inst. 31 (2007) 149-157.
[29] C.F. Goldsmith, S.J. Klippenstein, W.H. Green, Proc. Combust. Inst. 33 (2011) 273-282.
[30] E.R. Ritter, J. Bozzelli, Int. J. Chem. Kinet. 23 (1991) 767-778.
[31] S.W. Benson, Thermochemical Kinetics, 2nd ed. Wiley, New york, 1976.
[32] T.H. Lay, J.W. Bozzelli, A.M. Dean, E.R. Ritter, J. Phys. Chem. 99 (1995) 14514-14527.
[33] A. Amadio, M. Crofton, E. Petersen, Shock Waves 16 (2006) 157-165.
[34] Z. Hong, D.F. Davidson, R.K. Hanson, Shock Waves (2009) 331-336.
[35] R.J. Kee, F.M. Rupley, J.A. Miller, The Chemical Thermodynamic Data Base, Report No. SAND87- 8215B.UC-4, Sandia National Laboratory (1987).
[36] W.L. Flower, PhD Thesis, Stanford University, 1976.
[37] J.M. Hall, M. Rickard, E.L. Petersen, Combust. Sci. Technol 177 (2005) 455-483.
[38] H. Shen, J. Steinberg, J. Vanderover, M. Oehlschlaeger, Energy Fuels 23 (2009) 2482-2489.
[39] D. Healy, H.J. Curran, J.M. Simmie, D.M. Kalitan, C.M. Zinner, Barrett, AB, E.L. Petersen, G. Bourque, Combustion and Flame 155 (2008) 441-448.
[40] D. Healy, H.J. Curran, S. Dooley, J.M. Simmie, D.M. Kalitan, E.L. Petersen, G. Bourque, Combustion and Flame 155 (2008) 451-461.
[41] P. Dagaut, M. Cathonnet, J. Rouan, R. Foulatier, A. Quilgars, J. Boettner, F. Gaillard, H. James, Journal of Physics E: Scientific Instruments 19 (1986) 207-209.
[42] CHEMKIN-PRO 15112, Reaction Design, San Diego, 2012.
[43] M. Mehl, G. Vanhove, W. Pitz, E. Ranzi, Combust. Flame 155 (2008) 756-772.
[44] M. Mehl, J. Chen, W.J. Pitz, S.M. Sarathy, C.K. Westbrook, Energy Fuels 25 (2011) 5215-5223.
[45] M. Mehl, T. Faravelli, F. Giavazzi, E. Ranzi, P. Scorletti, A. Tardani, D. Terna, Energy Fuels 20 (2006) 2391-2398.
[46] S.S. Goldsborough, C. Banyon, G. Mittal, Combust. Flame 159 (2012) 3476-3492.
[47] S.S. Goldsborough, G. Mittal, C. Banyon, Proc. Combust. Inst. 34 (2013) 685-693.